

Gravitational Lens System as a Long Baseline Detector of Extremely Low Frequency Primordial Gravitational Wave

WENSHUAI LIU¹

¹*School of Physics, Henan Normal University, Xinxiang 453007, China*

ABSTRACT

The effect of extremely low frequency primordial gravitational wave with arbitrary direction of propagation on a non-aligned gravitational lens system is investigated. From the point of view of real astrophysical lens model, singular isothermal sphere lens model is adopted in the gravitational lens system. The results show that, under the perturbation from extremely low frequency primordial gravitational wave, time delay in the gravitational lens system could strongly deviate from that deduced from theoretical model. This means that the strongly deviate time delay could be the imprint of extremely low frequency primordial gravitational wave on gravitational lens system, indicating that gravitational lens system could be used as a long baseline detector to detect extremely low frequency primordial gravitational wave.

Keywords: gravitational lensing—gravitational waves

1. INTRODUCTION

Primordial gravitational waves (PGWs) with a nearly scale invariant spectrum (Abbott & Wise 1984; Starobinskii 1985; Rubakov et al. 1982; Fabbri & Pollock 1983; Starobinsky 1979; Sahni 1990; Allen 1988) are a robust prediction of inflation which not only leads to a flat, homogeneous, and isotropic Universe but also produces seed perturbations growing to create large scale structure in the Universe (Grishchuk 1976, 1977; Starobinsky 1980; Linde 1982). In order to confirm inflation and determine the energy scale of it, it is of great significance to detect PGWs. The traditional method of detection of PGWs with extremely low frequency in the range of 10^{-18}Hz - 10^{-16}Hz is the B-modes of polarization of cosmic microwave background (CMB) (Kamionkowski et al. 1997; Seljak & Zaldarriaga 1997). However, detection of PGWs with extremely low frequency using B-mode polarization faces challenges due to the foreground contamination from dust in our Milky Way. Thus, it is worth finding an alternative observational feature induced by such extremely low frequency PGWs.

Research in this work shows that gravitational lens system could act as a promising detector of extremely low frequency PGWs. The idea of using gravitational lens system to probe PGWs with extremely low frequency is proposed based on (Allen 1989, 1990; Frieman et al. 1994) where Allen (1989,

1990) suggested that gravitational lens system with a point mass lens could act as a detector of PGWs with extremely low frequency using time delays between different images of a quasar and, later on, study in Frieman et al. (1994) demonstrated that the method proposed by Allen (1989, 1990) could not work due to the fact that time delays induced by PGWs cannot be observationally distinguishable from the intrinsic time delays originating from the geometry of the gravitational lens system. Liu (2021a,b) prove that gravitational lens system with a point mass lens could detect extremely low frequency PGWs when the whole Einstein ring is taken into account. Both of Liu (2021a,b) and researches in (Allen 1989, 1990; Frieman et al. 1994) adopt an aligned gravitational lens system with a point mass lens. However, a point mass lens in strong gravitational lensing is unrealistic, the possibility of such aligned source-deflector-observer configuration is extremely low in the Universe and gravitational lens systems with a non-aligned configuration are common.

Recently, work of Liu (2022) proposes a new method to detect extremely low frequency PGWs using a non-aligned gravitational lens system with a point mass lens. It shows from Liu (2022) that time delay from a non-aligned gravitational lens system perturbed by extremely low frequency PGWs could deviate from the time delay deduced from theoretical model as much as 100 percent, meaning that gravitational lens system with a non-aligned configuration could serve as a possible long baseline detector of PGWs with extremely low frequency. However, the direction of propagation of PGWs adopted in Liu (2022) is not arbitrary and the lens is a point mass model.

In the general condition, the lens composes of a planar distribution of mass elements. In this work, from the point of view of real observation, we concentrate on the singular isothermal sphere (SIS) lens model frequently used in astrophysics and investigate the effect of extremely low frequency PGWs with arbitrary direction of propagation on a non-aligned gravitational lens system with a SIS lens. The results show that time delay with perturbation from extremely low frequency PGWs could strongly deviate from that deduced from theoretical model, indicating that a non-aligned gravitational lens system could be used as a long baseline detector of extremely low frequency PGWs.

2. PERTURBATIONS OF PGW ON GRAVITATIONAL LENS SYSTEM

We adopt a non-aligned gravitational lens system shown in Figure 1 where the projection of the source on the lens axis and the observer are not equidistant from the deflector. The source, the deflector and the observer are at $(x = L\beta, y = 0, z = -L)$, $(x = 0, y = 0, z = -AL)$ where $0 < A < 1$, and $(x = 0, y = 0, z = 0)$, respectively. The speed of light is set to be $c = 1$ and the metric of the gravitational wave with arbitrary direction of propagation is

$$h_{ij} = \frac{a_0}{a} [(u_i u_j - v_i v_j) h_+ + (u_i v_j + v_i u_j) h_\times] \times \cos(\omega\eta - \mathbf{k} \cdot \mathbf{x}) \quad (1)$$

where a is the scale factor and we set the present value $a_0 = 1$. z is in form of conformal distance and conformal time. The conformal time $\eta = t_e + (z + L)$ in order to approach the level of approximation, t_e is the time the photons were emitted at $(x = L\beta, y = 0, z = -L)$ so that ωt_e acts as the initial phase, $\mathbf{k} = \omega(\sin\theta \cos\phi, \sin\theta \sin\phi, \cos\theta)$ is the propagation vector, $\mathbf{u} = (\sin\phi, -\cos\phi, 0)$, $\mathbf{v} = (\cos\theta \cos\phi, \cos\theta \sin\phi, -\sin\theta)$, $\omega = 2\pi f$, f is the frequency of gravitational wave, h_+ and h_\times are the amplitude of the two polarizations of the gravitational wave, respectively.

With the gravitational potential of the deflector U , the total metric in the expanding universe is shown as

$$ds^2 = a^2(\eta) [(1+2U)d\eta^2 - (1-2U)(dx^2 + dy^2 + dz^2) - h_{ij} dx^i dx^j] \quad (2)$$

It shows from Baker & Trodden (2017) that the conformal time delay is equal to the physical time delay to an extremely good approximation. Thus, the following research is in terms of conformal distances and conformal times.

Then we can get the time of travel of light based on the equation given as (the detailed derivation is in Appendix A)

$$T \approx \int_{-L}^0 dz \left[1 + \frac{1}{2} \left(\frac{dx}{dz} \right)^2 + \frac{1}{2} \left(\frac{dy}{dz} \right)^2 + \frac{1}{2} h_{ij} \frac{dx^i}{dz} \frac{dx^j}{dz} - 2U \right] \quad (3)$$

From Eq. (3), $\frac{dx}{dz}$ and $\frac{dy}{dz}$ should be solved in order to calculate the time of travel of light perturbed by extremely low

frequency PGW with the same method shown in Frieman et al. (1994). To get $\frac{dx}{dz}$ and $\frac{dy}{dz}$, it should be noted that we drop the dependence on x and y in $\cos(\omega t - \mathbf{k} \cdot \mathbf{x})$ from Eq. (1) with explanation shown in Frieman et al. (1994) and the fourth term containing $\cos(\omega t - \mathbf{k} \cdot \mathbf{x})$ in Eq. (3) is the only place where x dependence should be included. Then we use equation shown as

$$\frac{\partial \mathbb{L}^2}{\partial x^\mu} - \frac{d}{dp} \left(\frac{\partial \mathbb{L}^2}{\dot{x}^\mu} \right) = 0 \quad (4)$$

where p is an affine parameter and

$$0 = \mathbb{L}^2 = a^2(\eta) [\dot{\eta}^2 - \dot{x}^2 - \dot{y}^2 - \dot{z}^2 - h_{11}\dot{x}^2 - h_{22}\dot{y}^2 - h_{33}\dot{z}^2 - 2h_{12}\dot{x}\dot{y} - 2h_{13}\dot{x}\dot{z} - 2h_{23}\dot{y}\dot{z}] \quad (5)$$

and we get $\frac{dx}{dz}$ and $\frac{dy}{dz}$ as follows when $z < -AL$ (the detailed derivation is in Appendix B)

$$\frac{dx}{dz} = \frac{d_2 a_1 - d_1 a_2}{a_2 b_1 - a_1 b_2} + \frac{c_1 a_2 - c_2 a_1}{a_2 b_1 - a_1 b_2} \quad (6)$$

$$\frac{dy}{dz} = \frac{d_2 b_1 - d_1 b_2}{a_1 b_2 - a_2 b_1} + \frac{c_1 b_2 - c_2 b_1}{a_1 b_2 - a_2 b_1} \quad (7)$$

where c_1 and c_2 are integration constants.

In order to obtain c_1 and c_2 , the details are as follows with fixed θ , ϕ , A and t_e . Based on the method of Fermat's principle shown in Frieman et al. (1994), after integrating Eq. (6) from $z = -L$ to $z = -AL$, the change in the direction of x-axis is

$$\Delta x_1 = \int_{-L}^{-AL} \frac{dx}{dz} dz = e_1 + c_1 f_1 + c_2 g_1 \quad (8)$$

where

$$e_1 = \int_{-L}^{-AL} \frac{d_2 a_1 - d_1 a_2}{a_2 b_1 - a_1 b_2} dz \quad (9)$$

$$f_1 = \int_{-L}^{-AL} \frac{a_2}{a_2 b_1 - a_1 b_2} dz \quad (10)$$

$$g_1 = \int_{-L}^{-AL} \frac{-a_1}{a_2 b_1 - a_1 b_2} dz \quad (11)$$

thus

$$x|_{z=-AL} = L\beta + \Delta x_1 \quad (12)$$

and the change in the direction of y-axis is

$$\Delta y_1 = \int_{-L}^{-AL} \frac{dy}{dz} dz = e_2 + c_1 f_2 + c_2 g_2 \quad (13)$$

where

$$e_2 = \int_{-L}^{-AL} \frac{d_2 b_1 - d_1 b_2}{a_1 b_2 - a_2 b_1} dz \quad (14)$$

$$f_2 = \int_{-L}^{-AL} \frac{b_2}{a_1 b_2 - a_2 b_1} dz \quad (15)$$

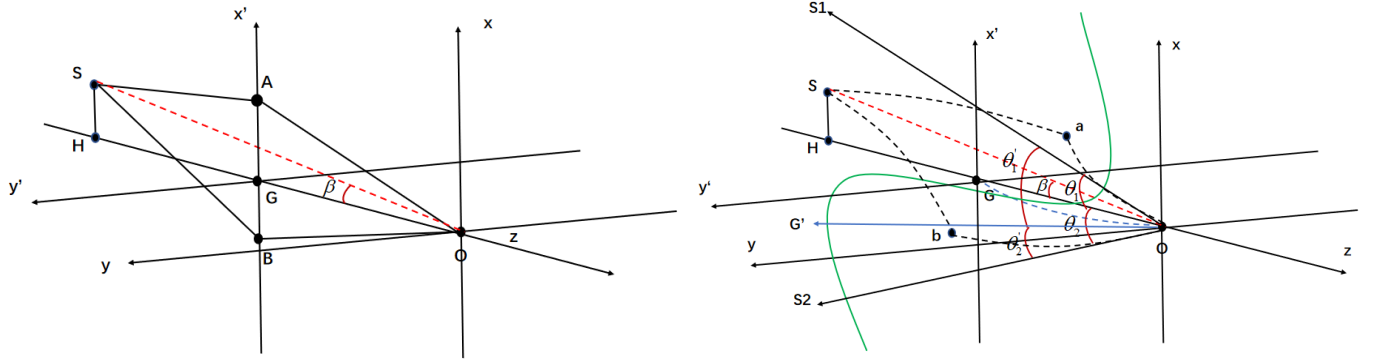


Figure 1. Left and right show the gravitational lens system. Right is perturbed by extremely low frequency PGW while there is no extremely low frequency PGW in the left. S, G, and O represent the source, the deflector, and the observer, respectively. H is the projection of the source on the line consisted of the observer and the deflector. The green curve in the right represents the extremely low frequency PGW traveling through the gravitational lens system. Under perturbation of extremely low frequency PGW, the dot curves in the right represent the trajectory of light emitted from the source and the deflector. a and b are in the $x' - y'$ plane where x' and y' are parallel to x and y , respectively. θ'_1 and θ'_2 represent the angular positions of the two observational image of the source. β is the angle between OS and OG.

$$g_2 = \int_{-L}^{-AL} \frac{-b_1}{a_1 b_2 - a_2 b_1} dz \quad (16)$$

so

$$y|_{z=-AL} = \Delta y_1 \quad (17)$$

When $z > -AL$, the geodesic equation of light is deflected at $z = -AL$ with a deflected angle α_x in the direction of x-axis and a deflected angle α_y in the direction of y-axis and

$$\alpha_x^2 + \alpha_y^2 = (2\eta)^2 \quad (18)$$

with relationship

$$\frac{\alpha_x}{\alpha_y} = \frac{x|_{z=-AL}}{y|_{z=-AL}} \quad (19)$$

which results from the fact that $\mathbf{R} = (x|_{z=-AL}, y|_{z=-AL}, 0)$, $\mathbf{a} = (\frac{dx}{dz}|_{z \rightarrow (-AL)^-}, \frac{dy}{dz}|_{z \rightarrow (-AL)^-}, 1)$ and $\mathbf{b} = (\frac{dx}{dz}|_{z \rightarrow (-AL)^+}, \frac{dy}{dz}|_{z \rightarrow (-AL)^+}, 1)$ are coplanar with relation $(\mathbf{R} \times \mathbf{a}) \cdot \mathbf{b} = 0$. Here, we set $2\eta = 4\pi (\frac{\sigma}{c})^2$ where σ is the stellar velocity dispersion of the lens galaxy.

The change in the direction of x-axis and y-axis are as follows when $z > -AL$

$$\Delta x_2 = \int_{-AL}^0 \frac{dx}{dz} dz = h_1 + c_1 i_1 + c_2 j_1 - \alpha_x L \quad (20)$$

$$\Delta y_2 = \int_{-AL}^0 \frac{dy}{dz} dz = h_2 + c_1 i_2 + c_2 j_2 - \alpha_y L \quad (21)$$

where

$$\frac{dx}{dz} = \frac{d_2 a_1 - d_1 a_2}{a_2 b_1 - a_1 b_2} + \frac{c_1 a_2 - c_2 a_1}{a_2 b_1 - a_1 b_2} - \alpha_x \quad (22)$$

$$\frac{dy}{dz} = \frac{d_2 b_1 - d_1 b_2}{a_1 b_2 - a_2 b_1} + \frac{c_1 b_2 - c_2 b_1}{a_1 b_2 - a_2 b_1} - \alpha_y \quad (23)$$

$$h_1 = \int_{-AL}^0 \frac{d_2 a_1 - d_1 a_2}{a_2 b_1 - a_1 b_2} dz \quad (24)$$

$$i_1 = \int_{-AL}^0 \frac{a_2}{a_2 b_1 - a_1 b_2} dz \quad (25)$$

$$j_1 = \int_{-AL}^0 \frac{-a_1}{a_2 b_1 - a_1 b_2} dz \quad (26)$$

$$h_2 = \int_{-AL}^0 \frac{d_2 b_1 - d_1 b_2}{a_1 b_2 - a_2 b_1} dz \quad (27)$$

$$i_2 = \int_{-AL}^0 \frac{b_2}{a_1 b_2 - a_2 b_1} dz \quad (28)$$

$$j_2 = \int_{-AL}^0 \frac{-b_1}{a_1 b_2 - a_2 b_1} dz \quad (29)$$

and we get

$$x|_{z=-AL} = -\Delta x_2 \quad (30)$$

$$\Delta y_1 = -\Delta y_2 \quad (31)$$

$$x|_{z=-AL}^2 + \Delta y_1^2 = R^2 \quad (32)$$

Combined with Eq. (18), Eq. (19), Eq. (30), and Eq. (31), the four unknowns c_1 , c_2 , α_x , and α_y are solved with two sets of solutions. Inserting c_1 and c_2 into Eq. (22) and Eq. (23), we get the angular positions of the two images as

$$\theta_{1x,2x} = -\frac{dx}{dz}|_{z=0} \quad (33)$$

$$\theta_{1y,2y} = -\frac{dy}{dz}|_{z=0} \quad (34)$$

However, from the point of view of real observation, the angular position of the image of the source is that with respect to the image of the deflector. To get the image angular position of the deflector, we use the same method described above. For the deflector, after integrating Eq. (6) and Eq. (7) from $z = -AL$ to $z = 0$, the change in the direction of

x-axis and in the direction of y-axis are

$$\Delta x' = \int_{-AL}^0 \frac{dx}{dz} dz = e_1 + c_1 f_1 + c_2 g_1 = 0 \quad (35)$$

$$\Delta y' = \int_{-AL}^0 \frac{dy}{dz} dz = e_2 + c_1 f_2 + c_2 g_2 = 0 \quad (36)$$

the two unknowns c_1 and c_2 with one set of solution are obtained, the angular position of the image of the deflector is given by inserting c_1 and c_2 into Eq. (6) and Eq. (7)

$$\theta_{dx} = -\left. \frac{dx}{dz} \right|_{z=0} \quad (37)$$

$$\theta_{dy} = -\left. \frac{dy}{dz} \right|_{z=0} \quad (38)$$

Thus, from the point of view of real observation, the image angular position of the source, which is the image of the source with respect to the image of the deflector, is shown as

$$\theta'_{1x,2x} = \theta_{1x,2x} - \theta_{dx} \quad (39)$$

$$\theta'_{1y,2y} = \theta_{1y,2y} - \theta_{dy} \quad (40)$$

The time delay $\Delta T_{Observation}$ based on Eq. (3) can be calculated. With the image positions from Eq. (39) and Eq. (40), the theoretical time delay ΔT_{Theory} can also be obtained as follows

$$\Delta T_{Theory} = 2\eta AL(-\theta'_1 + \theta'_2) \quad (41)$$

and $-\int_{-L}^0 U_1 dz + \int_{-L}^0 U_2 dz$ in $\Delta T_{Observation}$ could be expressed as

$$\begin{aligned} -\int_{-L}^0 U_1 dz + \int_{-L}^0 U_2 dz &= 2\eta AL \left(-\frac{R_1}{AL} + \frac{R_2}{AL} \right) \\ &= 2\eta(-R_1 + R_2) \end{aligned} \quad (42)$$

the obtained $\kappa = \frac{\Delta T_{Theory} - \Delta T_{Observation}}{\Delta T_{Theory}}$ could be the hint of extremely low frequency PGW.

In the case of $\theta = \frac{\pi}{2}$, $\phi = 0$, $h_\times = 0$ and h_+ is constant, the actual trajectory of light could be given in analytical form in details as

$$\frac{dx}{dz} = \gamma - \frac{1}{2}h \cos[\omega(t_e + z + L)] \quad (43)$$

$$\begin{aligned} x &= \gamma z - \frac{1}{2} \frac{h}{\omega} \sin[\omega(t_e + z + L)] + L\gamma + \frac{1}{2} \frac{h}{\omega} \sin(\omega t_e) \\ &\quad + L\beta \end{aligned} \quad (44)$$

for $z < -AL$ and

$$\frac{dx}{dz} = \gamma - \pm 2\eta - \frac{1}{2}h \cos[\omega(t_e + z + L)] \quad (45)$$

$$\begin{aligned} x &= \gamma z - \pm 2\eta z - \frac{1}{2} \frac{h}{\omega} \sin[\omega(t_e + z + L)] \\ &\quad + \frac{1}{2} \frac{h}{\omega} \sin[\omega(t_e + L)] \end{aligned} \quad (46)$$

for $z > -AL$ where

$$\begin{aligned} \gamma &= \pm 2\eta A + \frac{1}{2} \frac{h}{\omega L} \sin[\omega(t_e + L)] \\ &\quad - \frac{1}{2} \frac{h}{\omega L} \sin(\omega t_e) - \beta \end{aligned} \quad (47)$$

And we can also get the angular position of the image as follows

$$\theta_{1,2} = \pm 2\eta - \pm 2\eta A + \beta^* + \theta_0 \quad (48)$$

$$\theta'_{1,2} = \pm 2\eta - \pm 2\eta A + \beta^* \quad (49)$$

where

$$\beta^* = \beta + \beta_0 \quad (50)$$

$$\begin{aligned} \beta_0 &= \frac{1}{2} \frac{h}{\omega L} \sin(\omega t_e) - \frac{1}{2} \frac{h}{A\omega L} \sin[\omega(t_e + (1-A)L)] \\ &\quad + \frac{1-A}{2A} \frac{h}{\omega L} \sin[\omega(t_e + L)] \end{aligned} \quad (51)$$

and

$$\begin{aligned} \theta_0 &= \frac{1}{2} h \cos[\omega(t_e + L)] - \frac{1}{2} \frac{h}{A\omega L} \sin[\omega(t_e + L)] \\ &\quad + \frac{1}{2} \frac{h}{A\omega L} \sin[\omega(t_e + (1-A)L)] \end{aligned} \quad (52)$$

Thus, the observational magnification and theoretical magnification for image 1 and image 2 are given as

$$\mu_{1,2} = \frac{\theta_{1,2}}{\beta} \quad (53)$$

$$\mu'_{1,2} = \frac{\theta'_{1,2}}{\beta^*} \quad (54)$$

If only one image forms, the observational magnification is

$$\mu = \frac{\theta}{\beta} \quad (55)$$

Putting Eq. (43) to Eq. (46) into Eq. (3) and combining with Eq. (41) and Eq. (42), we can get κ .

The calculation of Eq. (39) and Eq. (40) shows that the positions of the two source images and the position of the lens image are collinear, thus, we set $\theta'_1 = \sqrt{\theta'^2_{1x} + \theta'^2_{1y}}$ and $\theta'_2 = \sqrt{\theta'^2_{2x} + \theta'^2_{2y}}$ which represent the positions of the two observational images.

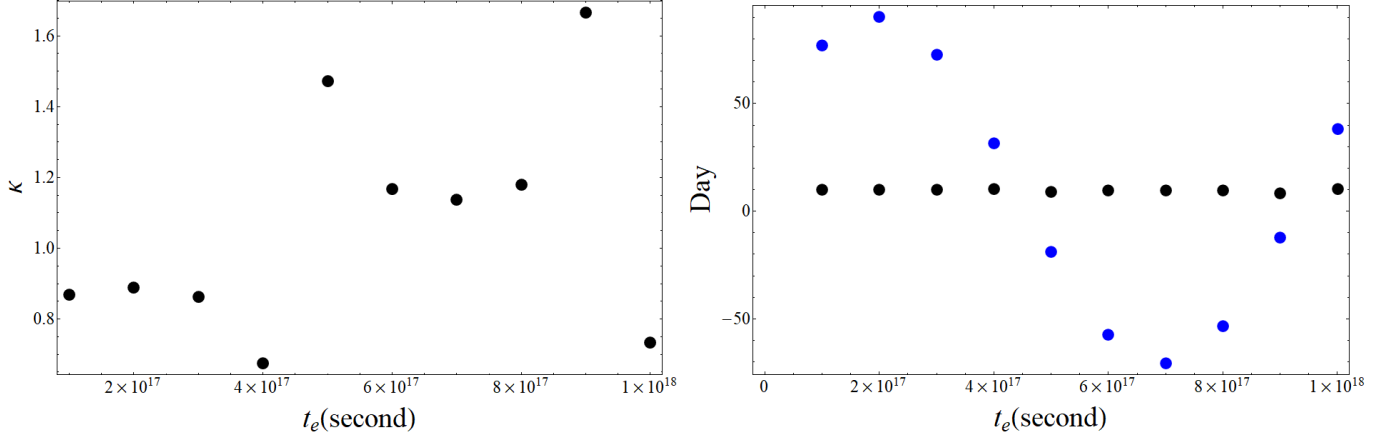


Figure 2. Left and right are κ and time delay along with t_e respectively. The black dots and the blue dots in the right represent the observational time delay and the theoretical time delay, respectively.

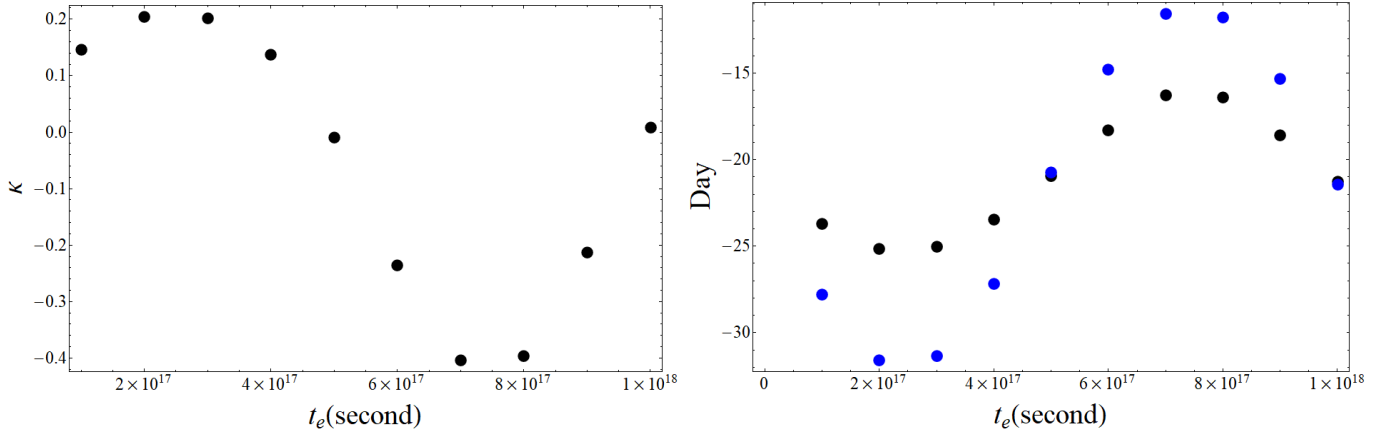


Figure 3. Left and right are κ and time delay along with t_e respectively. The black dots and the blue dots in the right represent the observational time delay and the theoretical time delay, respectively.

In the following calculations, we set $L = 8.4\text{Gpc}$ in form of conformal distance (corresponding to redshift equal to 6.4) and $A = 0.2$. The velocity dispersion in lens galaxy discovered is usually in the order of several hundred km/s , for instance, $\sigma \approx 323km/s$ in the len galaxy in RXJ1131-1231 (Suyu et al. 2013). We set $\eta = 6.7872 \times 10^{-6}$ corresponding to $\sigma \approx 310km/s$ in this work and $\beta = 0.2 \times 10^{-6}$. A , η , β and L can take other values and are not limited to the ones adopted here. The primordial spectrum of primordial gravitational wave is defined far outside of the horizon during inflation by (Wang et al. 2016)

$$h(k) = \Delta_t(k) = \Delta_R(k_0) r^{1/2} \left(\frac{k}{k_0}\right)^{\frac{n_t}{2} + \frac{1}{4}\alpha_t \ln(\frac{k}{k_0})} \quad (56)$$

where k_0 is a pivot conformal wavenumber and could be changed to a physical wavenumber through $k_0/a(\tau_H) = 0.05Mpc^{-1}$, $\Delta_R^2 = 2.1 \times 10^{-9}$ is the curvature perturbation determined by observartions, and $r \equiv \Delta_t^2(k_0)/\Delta_R^2(k_0)$ is the tensor-scalar ratio and $r < 0.032$.

When n_t and α_t are near 0, the primordial spectrum is nearly flat in the extremely low frequency range with $h \approx 8.1976 \times 10^{-6}$ when $r = 0.032$. According to research in (Chen et al. 2014; Wang et al. 2016; Wang & Zhang 2019; Zhang & Wang 2018), amplitude of primordial gravitational wave at frequency of $f = 10^{-18}Hz$ at present is about one order of magnitude lower than the primordial value. In the follows, we set r far lower that current upper limit of the tensor-scalar ratio in order to see whether or not primordial gravitational wave at frequency of $f = 10^{-18}Hz$ could affect gravitational lens system obviously.

In order to illustrate the effect of primordial gravitational wave at frequency of $f = 10^{-18}Hz$ on gravitational lens system with much lower tensor-scalar ratio than the current upper limit, we set $r = 0.001, 0.0001, 0.00001$, then, the current amplitude of primordial gravitational wave at frequency of $f = 10^{-18}Hz$ is $h = 1.4491 \times 10^{-7}, 4.5826 \times 10^{-8}, 1.4491 \times 10^{-8}$, respectively.

When $\theta \neq \frac{\pi}{2}$ and $\phi \neq 0$, the situation changes to the general case and there is only numerical result. Here, for simplicity, we set $\theta = 1.4$ and $\phi = 0.2$. With $h = 1.4491 \times 10^{-7}$, $f = 10^{-18}\text{Hz}$ and $A = 0.2$, we get κ along with t_e and observational and theoretical time delays in unit of day along with t_e in Figure 2 where it shows that the time delay observed can deviate from that predicted by theory obviously. The difference between the observational time delay and the theoretical time delay could reach near 80 days, meaning that PGWs with frequency $f = 10^{-18}\text{Hz}$ have significant effect on gravitational lens system. It should be noted that the results hold when the projection of the source is on the $y - z$ plane and not limited to the z -axis.

When primordial gravitational wave's frequency is equal to $f = 10^{-19}\text{Hz}$, its wavelength is larger than the horizon of the universe, resulting that such primordial gravitational wave is frozen and doesn't evolve. Only when the horizon size again is larger than its wavelength can it start oscillate and propagate. When $f = 10^{-19}\text{Hz}$, t in Eq. (1) is $t = t_e$. Then, with $\theta = 1.4$ and $\phi = 0.2$, $h = 1.4491 \times 10^{-6}$, $f = 10^{-19}\text{Hz}$ and $A = 0.2$, κ along with t_e and observational and theoretical time delays in unit of day along with t_e are shown in Figure 3.

In real observation, the observational time delay through dedicated and long-duration monitoring has uncertainties of a few percent (Tewes & Courbin 2013; Tewes et al. 2013). In addition, deep high-resolution imaging of the lensed arc could constrain the potential difference between different images at a few percent (Suyu et al. 2010). In order to break lensing degeneracy due to the lens galaxy mass distribution, the lens galaxy stellar velocity dispersion should be obtained. The line of sight weak lensing effect due to galaxies which are close in projection to the gravitational lens system along the line of sight needs to be inferred with independent observational data and could be constrained at about 5% level (Suyu et al. 2010). All of these sources of uncertainty are about 5% – 8% precision (Suyu et al. 2013). Furthermore, substructure in a precise model of the deflector potential could produce perturbation of a fraction of one day (Keeton & Moustakas 2009), and gravitational microlensing leads to perturbation with order of days if the source in the gravitational lens system is a quasar (Tie & Kochanek 2018). When time delay anomaly, which is usually observed in gravitational lensing, is larger than other perturbations described above, we may expect that we confirm the existence of extremely low frequency PGWs.

It shows from Hawkins (2021) that the observational time delay is about a year while time delay from prediction based on their mass model is about 410 days, thus, microlensing and substructure in the lens can't explain the difference of several tens of days. If other perturbations including the potential difference between different images, lens galaxy mass

distribution and line of sight weak lensing effect are inferred with independent observational data and such inferred perturbations couldn't reach several tens of days, there may exist the imprint of extremely low frequency PGWs on the gravitational lens system.

Primordial gravitational wave is isotropic statistically, meaning that the amplitude of primordial gravitational wave depends only on the frequency. Thus, we can average κ^2 over phase $\delta = \omega t_e$ and over 4π solid angle in the direction of \mathbf{k} to obtain the mean square as

$$\langle \kappa^2 \rangle = \int_0^{2\pi} \frac{d\delta}{2\pi} \int_0^{2\pi} \frac{d\phi}{2\pi} \int_0^\pi \frac{\sin\theta}{2} d\theta \kappa^2 \quad (57)$$

In order to get the expectation value of $\langle \kappa^2 \rangle$, we get the following with the same method as that in (Baskaran et al. 2006; Tong & Zhang 2009)

$$\langle \kappa^2 \rangle' = \int_0^{+\infty} \frac{\langle \kappa^2 \rangle}{f} df \quad (58)$$

A large $|\kappa|$ for a SIS lens is the hint of extremely low frequency PGWs.

3. CONCLUSIONS AND DISCUSSIONS

In order to find the possible hint of extremely low frequency PGWs in the Universe, the effect of extremely low frequency PGWs on time delay between different images of the source in a non-aligned gravitational lens system with SIS lens model is investigated in this work. It shows from this work that time delay between different images of the source in the non-aligned gravitational lens system could be strongly perturbed by extremely low frequency PGWs and may present obvious deviation from that deduced from theoretical model, meaning that a non-aligned gravitational lens system with SIS lens model could serve as a potential long baseline detector of extremely low frequency PGWs. Thus, in addition to B-mode polarization, obvious deviation of time delay in gravitational lensing could be used as alternative observational feature generated by extremely low frequency PGWs.

In addition to the condition that the deflector is a SIS gravitational deflector, it should be noted that this conclusion holds with the general condition that the deflector is not limited to a SIS gravitational deflector and can be general lens models. With lens model used in this work or the general lens model, the existence of extremely low frequency PGW may be confirmed if the time delay observed can strongly deviate from that predicted by theory including other perturbation described (for example, a precise model of the deflector potential across the images, the lens galaxy mass distribution, the line-of-sight weak lensing effect, substructure in the lens and gravitational microlensing). This work uses a single gravitational lens system to detect the hint of extremely low

frequency PGWs. In order to reduce the systematic uncertainty, Gravitational Lensing Array (GLA) which consists of many gravitational lens systems, can be adopted to detect the

existence of extremely low frequency PGWs. This is beyond the scope of this work and will be studied in future.

APPENDIX

A

With the metric of expanding universe and the perturbation from primordial gravitational wave

$$ds^2 = a^2(\eta)(1 + 2U)d\eta^2 - a^2(\eta)(1 - 2U)(dx^2 + dy^2 + dz^2) - a^2(\eta)h_{ij}dx^i dx^j \quad (1)$$

we get

$$d\eta = (1 + 2U)^{-\frac{1}{2}} \frac{1}{a} (\delta_{ij} a^2 (1 - 2U) dx^i dx^j + a^2 h_{ij} dx^i dx^j)^{\frac{1}{2}} \quad (2)$$

Combined with

$$dl = \sqrt{\delta_{ij} dx^i dx^j} \quad (3)$$

Eq. (2) changes to

$$d\eta = (1 + 2U)^{-\frac{1}{2}} ((1 - 2U) + h_{ij} \frac{dx^i}{dl} \frac{dx^j}{dl})^{\frac{1}{2}} dl \quad (4)$$

With

$$\frac{dz}{dl} = \cos \frac{\sqrt{dx^2 + dy^2}}{dz} \approx 1 - \frac{1}{2} \left(\frac{dx}{dz} \right)^2 - \frac{1}{2} \left(\frac{dy}{dz} \right)^2 \quad (5)$$

we have

$$dl = \left(1 + \frac{1}{2} \left(\frac{dx}{dz} \right)^2 + \frac{1}{2} \left(\frac{dy}{dz} \right)^2 \right) dz \quad (6)$$

Then

$$d\eta = dz \left(1 + \frac{1}{2} \left(\frac{dx}{dz} \right)^2 + \frac{1}{2} \left(\frac{dy}{dz} \right)^2 + \frac{1}{2} h_{ij} \frac{dx^i}{dz} \frac{dx^j}{dz} - 2U \right) \quad (7)$$

Finally, we get

$$T = \int_{-L}^0 d\eta = \int_{-L}^0 dz \left[1 + \frac{1}{2} \left(\frac{dx}{dz} \right)^2 + \frac{1}{2} \left(\frac{dy}{dz} \right)^2 + \frac{1}{2} h_{ij} \frac{dx^i}{dz} \frac{dx^j}{dz} - 2U \right] \quad (8)$$

B

Based on

$$\frac{\partial \mathbb{L}^2}{\partial x^\mu} - \frac{d}{dp} \left(\frac{\partial \mathbb{L}^2}{\dot{x}^\mu} \right) = 0 \quad (9)$$

and

$$\mathbb{L}^2 = a^2(\eta^2 - \dot{x}^2 - \dot{y}^2 - \dot{z}^2 - h_{11}\dot{x}^2 - h_{22}\dot{y}^2 - h_{33}\dot{z}^2 - 2h_{12}\dot{x}\dot{y} - 2h_{13}\dot{x}\dot{z} - 2h_{23}\dot{y}\dot{z}) \quad (10)$$

we get

$$\begin{aligned} a^2 \omega (h_{11}\dot{x}^2 + h_{22}\dot{y}^2 + h_{33}\dot{z}^2 + 2h_{12}\dot{x}\dot{y} + 2h_{13}\dot{x}\dot{z} + 2h_{23}\dot{y}\dot{z}) \sin(\omega\eta - \mathbf{k} \cdot \mathbf{x}) + \frac{da^2}{d\eta} L^2 &= \frac{d[a^2(2\dot{\eta})]}{dp} \\ a^2 \sin \theta \cos \phi \omega (h_{11}\dot{x}^2 + h_{22}\dot{y}^2 + h_{33}\dot{z}^2 + 2h_{12}\dot{x}\dot{y} + 2h_{13}\dot{x}\dot{z} + 2h_{23}\dot{y}\dot{z}) \sin(\omega\eta - \mathbf{k} \cdot \mathbf{x}) &= \frac{d[a^2(2\dot{x}h_{11} + 2\dot{y}h_{12} + 2\dot{z}h_{13} + 2\dot{x})]}{dp} \\ a^2 \sin \theta \sin \phi \omega (h_{11}\dot{x}^2 + h_{22}\dot{y}^2 + h_{33}\dot{z}^2 + 2h_{12}\dot{x}\dot{y} + 2h_{13}\dot{x}\dot{z} + 2h_{23}\dot{y}\dot{z}) \sin(\omega\eta - \mathbf{k} \cdot \mathbf{x}) &= \frac{d[a^2(2\dot{y}h_{22} + 2\dot{x}h_{12} + 2\dot{z}h_{23} + 2\dot{y})]}{dp} \\ a^2 \cos \theta \omega (h_{11}\dot{x}^2 + h_{22}\dot{y}^2 + h_{33}\dot{z}^2 + 2h_{12}\dot{x}\dot{y} + 2h_{13}\dot{x}\dot{z} + 2h_{23}\dot{y}\dot{z}) \sin(\omega\eta - \mathbf{k} \cdot \mathbf{x}) &= \frac{d[a^2(2\dot{z}h_{33} + 2\dot{x}h_{13} + 2\dot{y}h_{23} + 2\dot{z})]}{dp} \quad (11) \end{aligned}$$

Combined with Eq. (11), we have

$$a'_1 \dot{y} + b'_1 \dot{x} + d'_1 \dot{z} = c_1$$

$$a'_2 \dot{y} + b'_2 \dot{x} + d'_2 \dot{z} = c_2 \quad (12)$$

where

$$a'_1 = a^2(h_{22} \cos \phi + \cos \phi - h_{12} \sin \phi) \quad (13)$$

$$a'_2 = a^2(h_{22} \cos \theta + \cos \theta - h_{23} \sin \theta \sin \phi) \quad (14)$$

$$b'_1 = a^2(h_{12} \cos \phi - h_{11} \sin \phi - \sin \phi) \quad (15)$$

$$b'_2 = a^2(h_{12} \cos \theta - h_{13} \sin \theta \sin \phi) \quad (16)$$

$$d'_1 = a^2(h_{23} \cos \phi - h_{13} \sin \phi) \quad (17)$$

$$d'_2 = a^2(h_{23} \cos \theta - h_{33} \sin \theta \sin \phi - \sin \theta \sin \phi) \quad (18)$$

Then, based on Eq. (12), we get

$$\dot{x} = \frac{d'_2 a'_1 - d'_1 a'_2}{a'_2 b'_1 - a'_1 b'_2} \dot{z} + \frac{c_1 a'_2 - c_2 a'_1}{a'_2 b'_1 - a'_1 b'_2} \quad (19)$$

$$\dot{y} = \frac{d'_2 b'_1 - d'_1 b'_2}{a'_1 b'_2 - a'_2 b'_1} \dot{z} + \frac{c_1 b'_2 - c_2 b'_1}{a'_1 b'_2 - a'_2 b'_1} \quad (20)$$

With Eq. (11), we get

$$a^2(-\cos \theta \dot{\eta} + h_{33} \dot{z} + h_{13} \dot{x} + h_{23} \dot{y} + \dot{z}) = c_3 \quad (21)$$

then

$$a^2 \dot{\eta} (-\cos \theta + h_{33} \frac{dz}{d\eta} + h_{13} \frac{dx}{d\eta} + h_{23} \frac{dy}{d\eta} + \frac{dz}{d\eta}) = c_3 \quad (22)$$

Due to the fact that $|h_{33} \frac{dz}{d\eta} + h_{13} \frac{dx}{d\eta} + h_{23} \frac{dy}{d\eta}| \ll |-\cos \theta + \frac{dz}{d\eta}|$, thus,

$$a^2 \dot{\eta} = a^2 \frac{d\eta}{dp} = c_4 \quad (23)$$

With

$$\frac{dz}{d\eta} = 1 \quad (24)$$

we get

$$a^2 \frac{dz}{dp} = a^2 \frac{dz}{d\eta} \frac{d\eta}{dp} = c_4 \quad (25)$$

Then, Eq. (19) and Eq. (20) change to

$$\frac{dx}{dz} = \frac{d_2 a_1 - d_1 a_2}{a_2 b_1 - a_1 b_2} + \frac{c_1 a_2 - c_2 a_1}{a_2 b_1 - a_1 b_2} \quad (26)$$

$$\frac{dy}{dz} = \frac{d_2 b_1 - d_1 b_2}{a_1 b_2 - a_2 b_1} + \frac{c_1 b_2 - c_2 b_1}{a_1 b_2 - a_2 b_1} \quad (27)$$

where

$$a_1 = h_{22} \cos \phi + \cos \phi - h_{12} \sin \phi \quad (28)$$

$$a_2 = h_{22} \cos \theta + \cos \theta - h_{23} \sin \theta \sin \phi \quad (29)$$

$$b_1 = h_{12} \cos \phi - h_{11} \sin \phi - \sin \phi \quad (30)$$

$$b_2 = h_{12} \cos \theta - h_{13} \sin \theta \sin \phi \quad (31)$$

$$d_1 = h_{23} \cos \phi - h_{13} \sin \phi \quad (32)$$

$$d_2 = h_{23} \cos \theta - h_{33} \sin \theta \sin \phi - \sin \theta \sin \phi \quad (33)$$

REFERENCES

- Allen, B. 1989, Phys. Rev. Lett., 63, 2017
- Allen, B. 1990, Gen. Relativ. Gravit., 22, 1447
- Baskaran, D., Grishchuk, L. P., & Polnarev, A. G. 2006, PhRvD, 74, 083008
- Baker, T., & Trodden, M. 2017, PhRvD, 95, 063512
- Chen, J. W., et al. 2014, arXiv:1410.7151
- Ema, S. A., et al. 2022, MNRAS, 509, 3004
- Fabbri, R., & Pollock, M. D. 1983, Phys. Lett. 125B, 445
- Frieman J. A., Harari D. D., & Surpi G. C. 1994, Phys. Rev. D, 50, 4895
- Grishchuk, L. P. 1976, JETP Lett. 23, 293
- Grishchuk, L. P. 1977, Sov. Phys. Usp. 20, 319
- Hawkins, M. R. S. 2021, MNRAS, 503,3848
- Kamionkowski, M., Kosowsky, A., & Stebbins, A. 1997, PhRvL78, 2058
- Keeton, C. R., & Moustakas, L. A. 2009, ApJ, 699, 1720
- Linde, A. D. 1982, PLB 108, 389
- Liu, W. 2021a, Phys. Rev. D, 103, 103012
- Liu, W. 2021b, preprint (arXiv:2111.02404)
- Liu, W., 2022, MNRAS, 517, 2769
- Rubakov, V. A., Sazhin, M.V., & Veryaskin, A.V. 1982, Phys. Lett. 115B, 189
- Sahni, V. 1990, PhRvD42, 453
- Seljak, U., & Zaldarriaga, M. 1997, PhRvL78, 2054
- Starobinskii, A. 1985, Sov. Astron. Lett. 11, 133
- Starobinsky, A. A. 1979, JETP Lett. 30, 682
- Starobinsky, A. A. 1980, PLB 91, 99
- Suyu, S. H., Marshall, P. J., Auger, M. W., et al. 2010, ApJ, 711, 201
- Suyu, S. H., Auger, M. W., Hilbert, S., et al. 2013, ApJ, 766, 70
- Tewes, M., Courbin, F., & Meylan, G. 2013, A&A, 553, A120
- Tewes, M., Courbin, F., Meylan, G., et al. 2013, A&A, 556, A22
- Tie, S. S., & Kochanek, C. S. 2018, MNRAS, 473, 80
- Tong, M. L., & Zhang, Y. 2009, Phys. Rev. D, 80, 084022
- Wang, D.G., Zhang, Y., & Chen, J.W. 2016, Phys. Rev. D, 94, 044033
- Wang, B., & Zhang, Y. 2019, Res. Astron. Astrophys., 19, 024
- Zhang, Y., & Wang, B. 2018, J. Cosmol. Astropart. Phys., 11, 006